Highlights

Adaptive predictive control for peripheral equipment management to enhance energy efficiency in smart manufacturing systems

Miguel Angel Bermeo-Ayerbe, Carlos Ocampo-Martínez, Javier Diaz-Rozo

- Optimization-based control to manage peripheral equipment maximizing their efficiency.
- A continuous machine energy model adaptation scheme to react to its degradation.
- Experimental validation of control in a real industrial application via testbed.
- Energy efficiency performance comparison between adaptive and rule-based control.
- Results show that the proper management of peripheral equipment reduces energy costs.

Adaptive predictive control for peripheral equipment management to enhance energy efficiency in smart manufacturing systems

Miguel Angel Bermeo-Ayerbe[a,b,*], Carlos Ocampo-Martínez[a], Javier Diaz-Rozo[b]

[a] *Automatic Control Department, Universitat Politècnica de Catalunya, Institut de Robòtica i Informàtica Industrial (CSIC-UPC), Barcelona, Spain*
[b] *Aingura IIot, Donostia-San Sebastian, Spain*

Abstract

The importance of implementing energy efficiency methodologies in industrial environments has increased considerably in the last decade given the high energy costs and environmental impact (e.g., greenhouse gas emissions). This paper proposes a methodology to improve the energy efficiency of an industrial machine, without sacrificing either production or quality, using an adaptive predictive controller based on dynamic energy models that manages peripheral devices to activate/deactivate them at the proper times. The proposed adaptive mechanism aggregates robustness to the control system in industrial environments, which experiment constantly changes related to equipment degradation and that affect their energy consumption profile over time. Thus, this novel adaptive mechanism automatically updates the energy model to minimize the error between prediction and real energy consumption, including new energy behavior resulting from machine degradation. This methodology has been validated via a testbed and its performance was compared with rule-based control, which is the most widely used control strategy in industry. The energy efficiency of both approaches was evaluated using performance indicators, which show the effectiveness of the proposed control approach, highlighting remarkable improvements in reducing both

*Corresponding author

Email addresses: `miguel.angel.bermeo@upc.edu` (Miguel Angel Bermeo-Ayerbe), `carlos.ocampo@upc.edu` (Carlos Ocampo-Martínez), `jdiaz@ainguraiiot.com` (Javier Diaz-Rozo)

energy consumption (about 2%) and sudden power peaks (more than 11 %).

Keywords: Energy management systems, energy efficiency, manufacturing machines, model predictive control, adaptive control, subspace identification, Peripheral devices

---

1. Introduction

Efficient resource management helps reduce environmental impact and costs in manufacturing systems, which in turn contributes to a more sustainable society. Factors such as rising energy prices, legal environmental constraints, and incentives raise industry awareness, motivating companies to implement energy efficiency (EE) strategies [1]. Industry is one of the top consumers of energy in the world (around 42% in 2017), with a third of energy consumption corresponding to manufacturing [2]. In the last 40 years, the study, design, and development of energy management and EE strategies have led to a significant decrease in energy intensity, most especially in manufacturing [3].Nowadays, thanks to the rise of new Industry 4.0 and smart factory technologies, the implementation of energy management systems is easier, more accessible, and risk-free [4].

As the industrial machines are one of the main energy consumers and waste producers in a factory [5], in order to develop sustainable and efficient manufacturing, the maximization of their EE must be promoted [6, 7]. The basis for ensuring EE consumption in industrial machines is to design and build them using efficient devices and components, while the performance and EE of some devices (motors, air compressors, etc.) could be maximized using suitable control systems (e.g. variable speed drives) [5]. However, those measures are not enough to achieve overall machine efficiency, as proper synchronization between devices will lead to homogeneous consumption over time and better EE [6, 8]. Therefore, before incorporating a machine into an industrial production line, the activation/deactivation sequence of the devices should be optimized to achieve the required cycle time and EE consumption, considering process constraints and end-user efficiency requirements [9, 7]. When in operation, a wide variety of approaches can monitor the energy consumption of machine devices [10, 11]. Likewise, analyzing consumption and looking for energy inefficiencies can lead to the development of strategies to mitigate them [7, 12]. Other approaches have proposed a state-based consumption model with a graph-based optimization theory, which establishes

the optimal energy state sequence for given non-productive times [13, 14].

Since peripheral equipment may consume up to 70% of overall industrial machinery at full power [5, 15], various approaches have been proposed to manage this equipment; for instance, the EE of a cooling system improved through on-off control can reduce consumption by up to 25% [16]. Nonetheless, this kind of approach is only applicable to hot-gas bypass-type spindle cooling units with minimum thermal fluctuations. Activation/deactivation criteria established for peripheral equipment during standby states can reduce energy waste [17]. Other methodologies use kinetic energy recovery systems to feed peripheral equipment and an offline energy estimation tool to detect deficiencies [18, 19]. Since some peripheral equipment items support several machines, approaches are oriented to energy management of production chains [20, 21]. Although these approaches work well in specific scenarios, energy models generally require a more granular approach to allow better visibility of the process chain. Since the models used are static, they do not consider the dynamic behavior of real manufacturing facilities, losing important information during non-stationary states, such as on power spikes. Hence, the approach proposed in this paper outperforms previously reported works in establishing a structured methodology based on state-space realizations that adequately represents the dynamic behavior of the energy consumption for a manufacturing machine. This proposed methodology is properly integrated into a modular management scheme for such systems towards the statement of a smart manufacturing architecture.

The main contribution of this work is a methodology to manage peripheral equipment in real time using an adaptable data-driven model. This methodology increases the EE of a machine during the production cycle by managing the time-varying energy consumption of peripheral equipment, subject to known periodic and fixed energy demand given by the devices associated with the periodic process. Regarding the last devices, they are defined as synchronous devices with optimally defined schedules to perform the process correctly in terms of time and energy. Therefore, the proposed approach ensures that the overall machine consumption is as homogeneous as possible, avoiding peaks above the contracted electric power capacity and hopefully reducing the electric consumption. Moreover, production and quality will not be affected since the process configuration is not modified.

The proposed methodology consists of a strategy to generate data-based energy models with high fitting, a adaptive mechanism online, and a control law based on real time optimization with system behavior prediction

capabilities. The adaptive mechanism is proposed to consider changes in the dynamics of energy consumption over time, caused by machine degradation from continuous use. Whilst earlier approaches cannot react to new environmental conditions (e.g., temperature, humidity, tool) and equipment deterioration, which affects the performance of the machine and change its consumption profile [19, 22]. Thus, with the proposed approach, the energy model is automatically updated, reacting to changes in the energy consumption profile of the machine and the environment, reducing the error between model consumption prediction and real machine consumption. This methodology offers reliability and robustness, as the controller always makes decisions from a valid energy model in relation to current energy consumption by the machine.

For the validation of the proposed approach, a testbed was used to emulate the energy profiles of an industrial machine. This testbed is certificated by the Industrial Internet Consortium (IIC) [23] and its objective is to validate Industrial Internet of Things (IIoT) technologies for smart factories[1]. The validation procedure compared the performance of the proposed approach with a rule-based control (RBC) in three different scenarios, whose performance was measured by using four key performance indicators (KPIs). Based on the results, the potential of the proposed approach is demonstrated, as it yields improvements in EE in terms of energy savings and reductions in power peaks.

The structure of this paper is summarized as follows: In Section 2, the testbed and the strategy to emulate the consumption profiles of industrial machines are described. Section 3 raises the industrial process emulated using the testbed to validate the proposed methodology. Section 4 details the peripheral management methodology to improve EE of industrial machines. The validation process and results are presented in Section 5, in which the benefits of using the proposed control strategy are demonstrated. Finally, in Section 6, the main conclusions are drawn.

2. Testbed

Due to the high complexity and cost of performing tests on industrial machines, part of the testbed was designed and built to emulate the energy

[1] `https://hub.iiconsortium.org/smart-factory-machine-learning`

consumption behavior of a manufacturing machine. As shown in the diagram in Figure 1, the testbed activates/deactivates devices to create consumption profiles. The red lines represent electrical connections and the blue lines are either data transfer channels or control signals. The devices used to build energy profiles are two three-phase motors, a heater, and two uninterruptible power supplies (UPS). In order to manage the UPS energy consumption (as a security device that stores energy), each UPS supplies energy to two loads: to a fan plus a lamp, and to two fans. Connected between the UPS and the loads is an alternating current (AC) regulator that limits the current to the loads, thereby regulating the energy consumption of each UPS. The other devices are controlled through a variable-frequency drive for a three-phase motor and relays for the heater and the other motor. Note that the relay actuators only allow devices to be activated or deactivated, while other actuators allow energy consumption to be regulated.

The embedded system (ES) is an Aingura Insights (AI) with a Zynq® Ultrascale+™ MPSoC, which is used in industry for data acquisition and processing (i.e., an IIoT computing edge device). The ES executes the main control logic to decide which devices should be activated/deactivated (emulating the role of a programmable logic controller (PLC)), and through the user datagram protocol (UDP), sends commands to the low-level control devices to generate analog/digital signals to the actuators that establish decisions made. An Arduino Leonardo (AL) and a WEB LAN IP ethernet relay controller (WLIE-RC) are used as low-level controllers. Regarding the AL, this generates a pulse-width modulation (PWM) signal, which configures the actuator and allows a duty cycle to be established between the 0 and 255 logic levels. The energy consumption spectrum of those AL-governed devices therefore has 256 logic levels, 0 when the device is fully off and 255 when energy consumption is maximum. Although low-level controllers do not have the same industrial robustness as a computer numeric control (CNC), but for the scope of this research, both AL and WLIE-RC operate with adequate scan cycle and especially AL has scan cycle (microseconds) comparable to that of a CNC.

The energy sensor is a combination of AI and industrial clamp meters to measure five energy signals (voltage, current, active power, reactive power and apparent power) for each electrical phase, with a sampling frequency between 4 and 8 kHz. In this case, the sensor was configured at 4 kHz to have a sample every 250 μs. Each second the sensor transmits a set of last-second measurements to the ES, i.e., each second the ES receives a set of

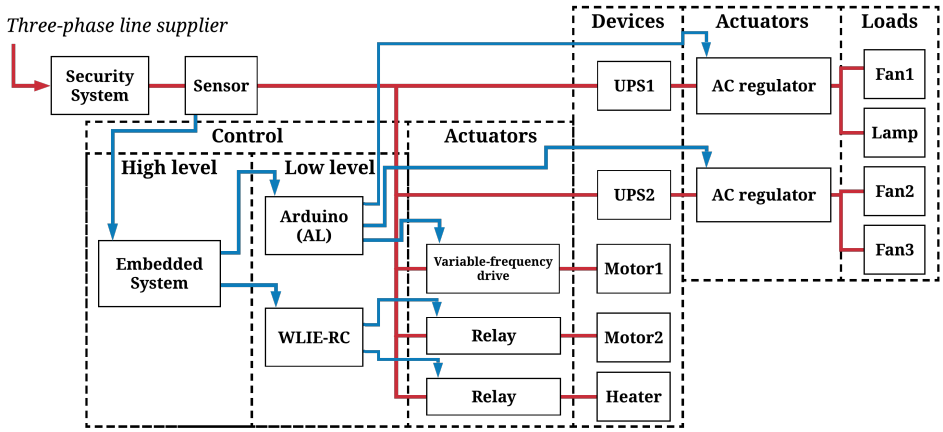

Figure 1: The testbed block diagram.

4000 energy measurements corresponding to the total energy consumption of the testbed. All single-phase devices (e.g., UPS and heater) were connected to the B phase, so most of the electrical profiles shown are from the B phase.

3. Case study

The energy consumption of a manufacturing process, called electro-discharge machining, was emulated using the testbed. For this use-case, the process is performing two cutting operations on a workpiece. The energy profiles of the machining process and the peripheral devices are presented in Figure 2, where the peripheral device profiles are independent of the machining process, to illustrate their energy consumption behavior for different input values. The periodic consumption produced by the process is the result of combining the heater (D_{s_1}) and UPS1 (D_{s_2}), which is shown in Figure 2a with a period of $T_{mp} = 29$ s. Based on previous work [24], the main machine process is assisted by the following three peripheral systems:

(i) *Air-supply pump.* For the pneumatic actuators to work properly, this pump must maintain pressure conditions in the accumulator. The three-phase Motor1 (D_{p_1}) represents the energy consumption of this pump, as shown in Figure 2b. The dynamic model of the accumulator

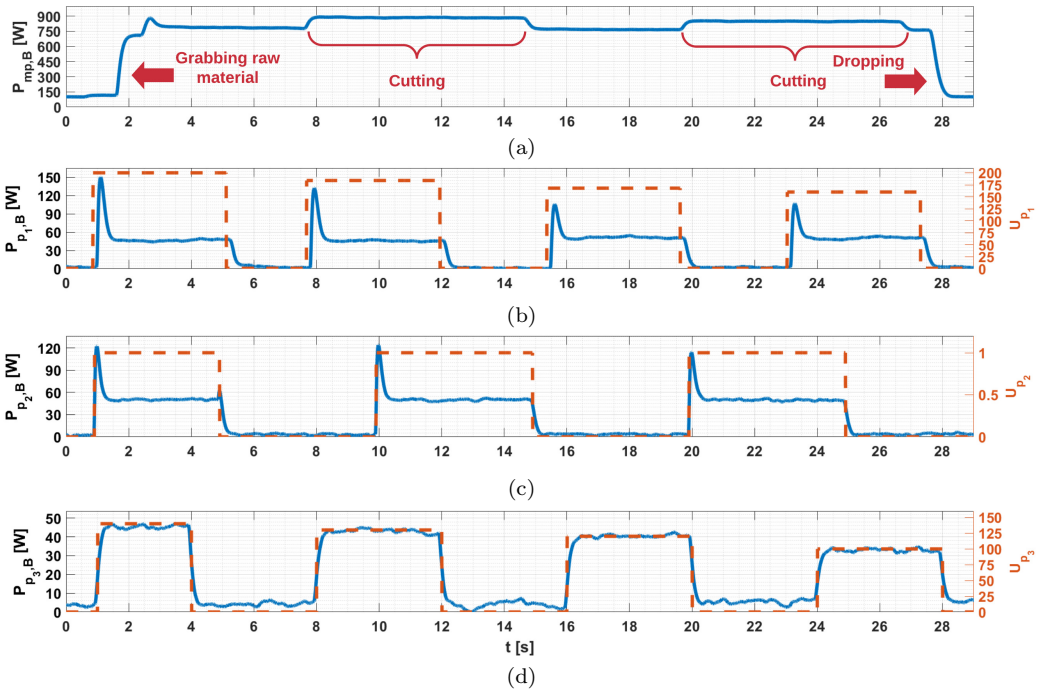

Figure 2: Energy consumption profile for the machining process and peripheral devices (dashed lines indicate the set input value): (a) shows the energy consumption during a period of the machining process, from grabbing the raw material, removing the material to releasing the workpiece. (b) and (d) display the energy profiles for different speed conditions of the air pump and the coolant recirculation pump, respectively. (c) shows the on-off power consumption of the hydraulic pump.

was proposed in the following way:

$$q_1(k+1) = q_1(k) + \begin{bmatrix} M_{in_{air}} & -M_{out_{air}} \end{bmatrix} \begin{bmatrix} u_{p_1}(k) \\ u_{s_1}(k) \end{bmatrix}, \tag{1a}$$

$$y_{q_1}(k) = q_1(k) \frac{R\ T}{V_T\ W_M} + P_{atm}, \tag{1b}$$

$$\underline{y_{q_1}} \leq y_{q_1} \leq \overline{y_{q_1}}, \tag{1c}$$

being $q_1 \in \mathbb{R}$ the mass and $y_{q_1} \in \mathbb{R}$ the pressure inside the accumulator with an operating range of $\underline{y_{q_1}} = 500000$ Pa to $\overline{y_{q_1}} = 750000$ Pa. The model constants are defined as $M_{out_{air}} = 1.5 \times 10^{-3}$ m^3/s the air discharge coefficient, $M_{in_{air}} = 2.5 \times 10^{-3}$ m^3/s the coefficient of recharging air, $R = 8.314472$ Jk^{-1}mol^{-1} the gas constant, $T = 298.15$ K the environmental temperature, $V_T = 5 \times 10^{-3}$ m^3 the tank volume, $W_M = 28.966 \times 10^{-3}$ kg/mol the molecular weight and $P_{atm} = 101325$ Pa the

value of an atmosphere. The input pump u_{p_1} operates between 160 and 200 logic levels, and the input $u_{s_1} \in \{0, 1\}$ is associated with the pressure losses when the D_{s_1} is activated. The control rule established for this pump is to enable the pump when the pressure y_{q_1} is near the lower bound $\underline{y_{q_1}}$, then the pump is activated with a maximum speed (200 logical level) until the upper bound $\overline{y_{q_1}}$ is reached.

(ii) *Hydraulic pump.* Similarly to the air-supply pump, the machine has a hydraulic pump to supply flow with enough power to meet the pressure demanded by hydraulic actuators. The energy profile of the three-phase Motor2 (D_{p_2}) is used as the consumption profile of the hydraulic pump, as displayed in the Figure 2c. The hydraulic system was modeled as

$$q_2(k+1) = q_2(k) + M_{in_{press}} u_{p_2}(k) - M_{out_{press}}, \tag{2a}$$

$$y_{q_2}(k) = q_2(k), \tag{2b}$$

$$\underline{y_{q_2}} \leq y_{q_2} \leq \overline{y_{q_2}}, \tag{2c}$$

where $q_2, y_{q_2} \in \mathbb{R}$ are the accumulator pressure, $M_{in_{press}} = 5$ bar the pump inlet pressure, $M_{out_{press}} = 3$ bar the pressure losses of the accumulator and $u_{p_2} \in \{0, 1\}$. The control rule is to keep the accumulator pressure within a range of $\underline{y_{q_2}} = 50$ bar to $\overline{y_{q_2}} = 150$ bar through an on-off control.

(iii) *Coolant-supply pump.* The coolant system maintains proper machining conditions, reducing the high temperature and removing the eroded particles between the workpiece and the electrode. Through a recirculation pump system, the dirty coolant is filtered and transferred to the clean tank for reuse. The consumption profile of this system is emulated by UPS2 (D_{p_3}) and is shown in the last row in Figure 2d. The dynamic model of this system is presented as follows:

$$\begin{bmatrix} q_{3,1}(k+1) \\ q_{3,2}(k+1) \end{bmatrix} = \begin{bmatrix} q_{3,1}(k) \\ q_{3,2}(k) \end{bmatrix} + \begin{bmatrix} z_1 & \frac{-M_{tp1}}{A_c\ \rho_c} \\ -z_1 & \frac{M_{tp2}}{A_d\ \rho_c} \end{bmatrix} \begin{bmatrix} u_{p_3}(k) \\ u_{s_2}(k) \end{bmatrix}, \tag{3a}$$

$$z_1 = \frac{\eta}{(A_d\ \rho_c)(H_{t1 \to t2}\ \rho_c + \Delta P_{filter})}, \tag{3b}$$

$$\begin{bmatrix} y_{q_{3,1}}(k) \\ y_{q_{3,2}}(k) \end{bmatrix} = \begin{bmatrix} q_{3,1}(k) \\ q_{3,2}(k) \end{bmatrix}, \tag{3c}$$

$$\underline{q_{3,1}} \leq q_{3,1} \leq \overline{q_{3,1}}, \tag{3d}$$

$$\underline{q_{3,2}} \leq q_{3,2} \leq \overline{q_{3,2}}, \tag{3e}$$

with $q_{3,1} \in \mathbb{R}$ and $q_{3,2} \in \mathbb{R}$ the level in the clean tank and dirty tank, respectively. The bounds are $\underline{q_{3,1}} = 0.3$ m, $\underline{q_{3,2}} = 0.6$ m, $\overline{q_{3,1}} = 0.5$ m and $\overline{q_{3,2}} = 0.8$ m. The model constants are defined as $A_c = 0.0314$ m^2 the clean tank area, $A_d = 0.0314$ m^2 the dirty tank area, $\rho_c = 1042.48$ kg/m^3 the coolant density, $\eta = 0.85$ the efficiency of pump, $H_{t1 \to t2} = 0.6$ the energy losses by friction, $\Delta P_{filter} = 1000$ Pa the filtering coefficient and, $M_{tp1} = 11 \times 10^{-3}$ and $M_{tp2} = 9.1 \times 10^{-3}$ are constants associated with the coolant flow required. The input pump operates u_{p_3} with inputs between 100 and 140 logic levels, and the input $u_{s_2} \in \{0, 1\}$ associated with device D_{s_2} indicating when clean coolant is used. The control rule for this system is to activate the pump (at full speed $u_{p_3} = 200$) when the dirty coolant reaches maximum level $\overline{q_{3,2}}$, then all the dirty coolant will filter and transfer to a clean tank until the dirty coolant level reaches a minimum $\underline{q_{3,2}}$ allowed.

4. Proposed approach

4.1. Energy models

Traditional methodologies to determine mathematical models imply an exhaustive procedure and are exclusively focused on a particular machine or device. However, this paradigm is changed due to the boom in technology that allows real-time monitoring and measurement of energy consumption. System identification (SI) methodologies, which generate control-oriented models based on measurements [25, 26], allow an interface to be created that applies the theory of control to real-world scenarios, reducing modeling efforts. The model is determined by observing input and output measurements only, without using physical laws.

A previous work proposed a methodology for identifying energy models via subspace identification (Sub-ID) algorithms [27]. This methodology is oriented to the identification of multiple-input and multiple-output (MIMO) systems, given that a machine may have several devices to consider. Therefore, each activation of device is used as model inputs and the energy consumption information used as outputs. Note that the number of outputs may vary depending on the energy sensor or the electrical phases to consider; in this case, a three-phase line is used. The approach used here is state-space identification based on the Hankel matrix created with an input-output identification dataset. This matrix performs as a regressive matrix that solves a least-squares problem, given the linear combination of subspace matrices

that describe the data. The state-space matrices are computed through the decomposition of the subspace matrices, using reliable and widely known and available numerical algorithms. As a result, the following discrete linear time-invariant state-space model is obtained:

$$x(k+1) = A\ x(k) + B\ u(k) + \omega(k), \tag{4a}$$

$$y(k) = C\ x(k) + D\ u(k) + \upsilon(k), \tag{4b}$$

being $u \in \mathbb{R}^m$, $y \in \mathbb{R}^l$ and $x \in \mathbb{R}^n$ vectors at discrete-time instant k of the m inputs, l outputs and n states (i.e., the model order) of the system, respectively. Furthermore, $A \in \mathbb{R}^{n\times n}$ the system matrix that describes the dynamics of the system, $B \in \mathbb{R}^{n\times m}$ the input matrix that represents a linear transformation of the current input in the contribution to the next state, $C \in \mathbb{R}^{l\times n}$ the output matrix that describes the effect of current states on outputs, $D \in \mathbb{R}^{l\times m}$ the feedthrough (or feedforward) matrix allows modeling when there is a direct influence of the input over the measurements, $\omega \in \mathbb{R}^n$ and $\upsilon \in \mathbb{R}^l$ are non-measurable vector signals that affect the states and measures, respectively.

In general, real systems have intrinsic input-output delays associated with data transmission and processing. Although this algorithm supports those delays with a high-order model, it is recommended to shift the input to remove those delays. Thus, the model accuracy is enhanced while avoiding increasing its order. Finally, following this identification procedure, a discrete linear time-invariant energy model is generated with a low fitting error with respect to real behavior and with a low model order, also potentially useful for the design of reliable and reactive controllers. State-space models are widely used in the design of modern control strategies, with numerous industrial processes already described with great precision [28].

For the purposes of this research, an offline model was identified using an identification dataset, and a second dataset was used to validate model performance. As shown in Figure 3, the generated model has a high fit rate with respect to the measurements: it only applies the input sequences and compares the outputs with the measurements (without any feedback). The calculated fit rate is defined as the complement of the normalized root mean squared errors [29], i.e.,

$$\gamma(S, \hat{S}) = 100\ \max\left(1 - \frac{\|S - \hat{S}\|_2}{\|S - \mu_S\|_2}, 0\right)\%, \tag{5}$$

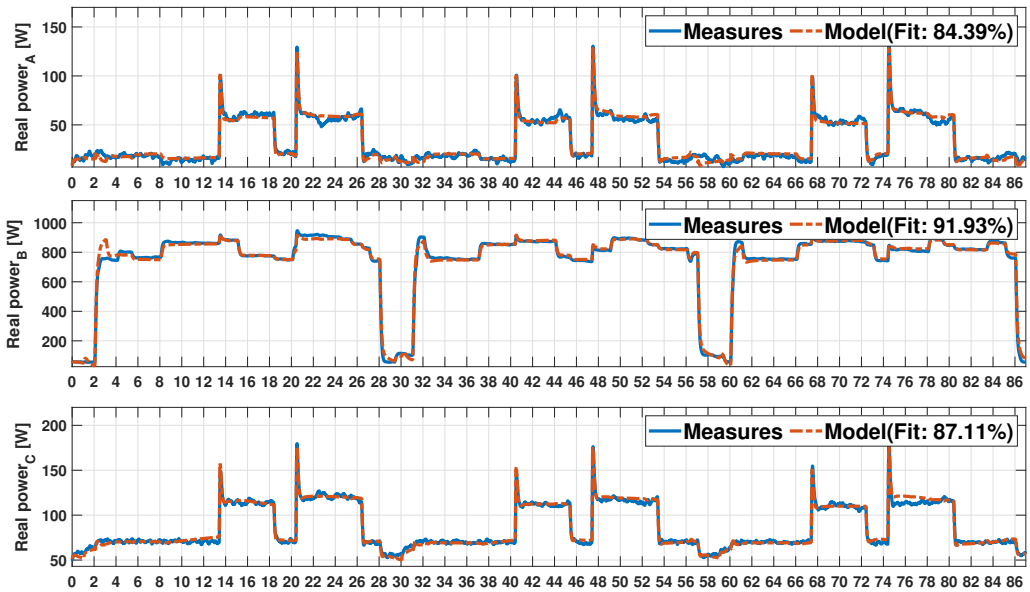

Figure 3: Comparison between the validation data (three machine cycles) and the model estimation.

where S is the energy consumption measurement, μ_S the mean measured consumption and $\hat{S}$ the estimated consumption. The model demonstrates the ability of the Sub-ID algorithm to generate highly accurate energy models (greater than 80%). Note that the results may depend on the system and its non-linearities.

4.2. Optimization-based control

In manufacturing processes, machinery is constituted by synchronous and peripheral devices that are controlled via two subsets of discrete inputs U_s and U_p, respectively. Both types of inputs form the input vector of the control system

$$U = \begin{pmatrix} U_s \\ U_p \end{pmatrix}. \tag{6}$$

Therefore, as a notation, the subscripts $\bullet_s$ and $\bullet_p$ are used to refer to the matrices of synchronous devices and peripheral devices, respectively. The periodic process is predefined with a fixed, known and periodic activation sequence of U_s, with a machine period (T_{mp}) that must be synchronized

with other machines involved in the production line. Peripheral devices perform auxiliary tasks to maintain, cool, clean and ensure correct operation of the machine. The activation/deactivation of U_p depends on sensors and/or timers, e.g., the pressure in a pneumatic system. Thereby, peripheral equipment control law must guarantee that the values of the sensors comply with the defined operating ranges, ensuring the proper conditions of the machine. Dynamic models, called q-relations, are used to estimate the behavior of peripheral systems, which indicate the impact of U_p on sensor values.

The only energy sensor installed in the machine provides real-time measurements of energy consumption (S) for the entire machine, including synchronous, peripheral, passive, and unknown devices. Passive devices, which have constant consumption, are frequently seen as an offset in electrical signals, e.g., actuators, sensors, and embedded systems, while unknown devices refer to the inputs of devices that are unknown to the controller. Figure 4a depicts the inputs and outputs considered in the control problem.

Due to the periodic and fixed nature of the process, the diverse constraints imposed by the process and device operation modes, a model predictive control (MPC) strategy is proposed to manage the peripheral devices. Based on the previously identified model, the following finite-time open-loop optimization problem is stated:

$$\min_{\mathfrak{U}(k)} \hat{\mathbf{S}}_s(k)\hat{\mathbf{S}}_p(k)^T \tag{7a}$$

subject to

$$\hat{x}_p(k|k) = \hat{x}_{p,0}(k), \tag{7b}$$
$$\hat{x}_p(k+k_h+1|k) = A\ \hat{x}_p(k+k_h|k) + B_p\ U_p(k+k_h|k), \tag{7c}$$
$$\hat{S}_p(k+k_h|k) = C\ \hat{x}_p(k+k_h|k) + D_p\ U_p(k+k_h|k), \tag{7d}$$
$$q(k+k_h+1|k) = f_q(q(k+k_h|k), U_p(k+k_h|k), U_s(k+k_h|k), \tag{7e}$$
$$Y_q(k+k_h|k) = h_q(q(k+k_h|k)), \tag{7f}$$
$$U_p(k+k_h|k) \in \mathbb{U}_p, \tag{7g}$$
$$q(k+k_h|k) \in \mathbb{Q}, \tag{7h}$$

where (7b) is the initial condition that will change at each sampling time, (7c) and (7d) reflect the energy model considering only the inputs of the peripheral devices, (7e) and (7f) are dynamic models of the q-relations, and

(7g) and (7h) are constraints related to the device inputs domain and states of q-relations, respectively. Depending on the actuator, the inputs domain may be a binary domain (on/off) or a range of values that allow establishing a connection with the power consumption level of the equipment (from low to high levels).

The objective function (7a) seeks the optimal future sequence of peripheral devices inputs

$$\mathfrak{U}(k) \triangleq \{U_p(k|k), \ldots, U_p(k+H_p|k)\}$$

along the prediction horizon H_p to obtain the most efficient total consumption. This goal is achieved by dividing the estimated total future consumption into

$$\hat{\mathbf{S}}_s(k) = \begin{bmatrix} \hat{S}_s(k|k) & \hat{S}_s(k+1|k) & \cdots & \hat{S}_s(k+H_p|k) \end{bmatrix}$$

and

$$\hat{\mathbf{S}}_p(k) = \begin{bmatrix} \hat{S}_p(k|k) & \hat{S}_p(k+1|k) & \cdots & \hat{S}_p(k+H_p|k) \end{bmatrix},$$

corresponding to estimates of the future energy consumption from synchronous and peripheral devices, respectively. Besides, $\hat{\mathbf{S}}_s(k)$ is computed beforehand to solve the problem, using the model and the future sequence of synchronous device inputs that are always known. In this way, $\hat{\mathbf{S}}_s(k)$ act as weights to penalize activation in high-energy consumption instants; thus, weights will be higher when a peripheral device is activated in the same instant as a synchronous device than when activated when all synchronous devices are deactivated. The resulting linear objective function does not require tuning parameters and has low computational complexity.

The current states of the model and the energy consumption $\hat{\mathbf{S}}_s(k)$ of the synchronous devices are estimated and used as the initial condition in the optimization problem (7) that is solved in each second. Thus, from the computed optimal sequence $\mathfrak{U}^*(k)$, only the inputs of the first step $U_p(k) = U_p^*(k|k)$ are applied to the peripheral devices while the rest of the sequence is discarded [30]. The current states of the devices according to the models can be estimated by an observer and the block diagram of the proposed control system using such a proposed observer is shown in Figure 4b.

4.3. Adaptive mechanism

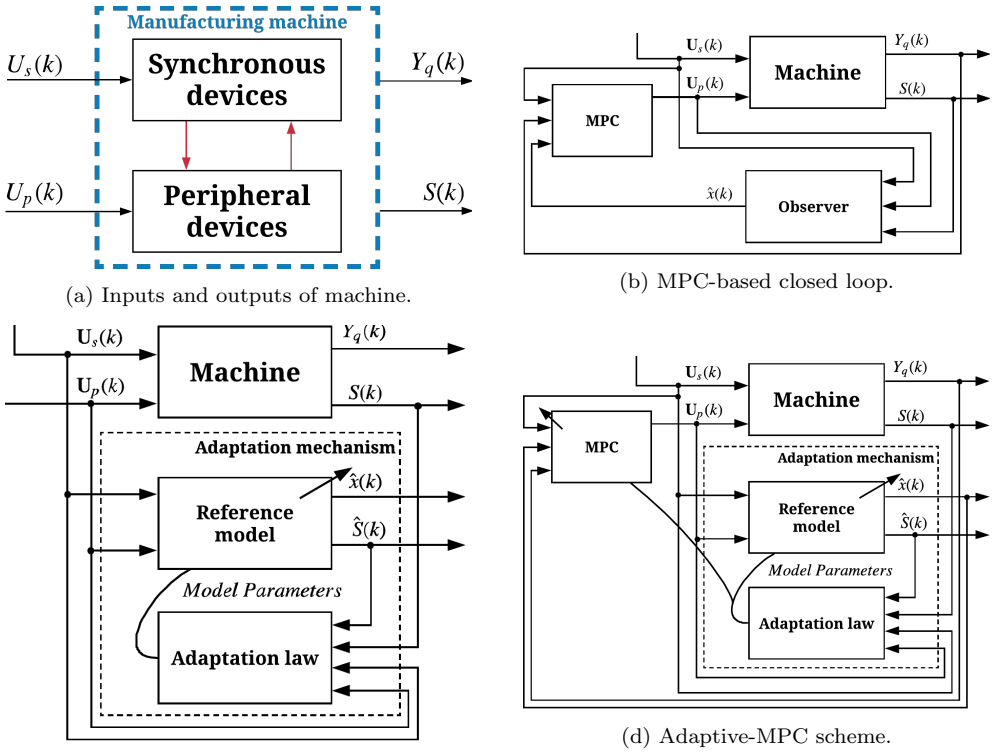

(a) Inputs and outputs of machine.

(b) MPC-based closed loop.

(c) Adaptive scheme.

(d) Adaptive-MPC scheme.

Figure 4: Block diagrams related to the proposed approaches.

The energy consumption profiles of devices change over time due to degradation resulting from constant use in an industrial environment. Figure 4c depicts an online adaptation scheme to fit the energy model with new energy consumption behaviors. The reference model is initialized using a model identified offline and used to estimate the machine consumption, which is compared with real energy consumption in the adaptation law block. This block generates a new model in each $N_{T_{mp}}$ machine period, using the S, $\mathbf{U}_s$, and $\mathbf{U}_p$ signals stored in the previous $N_{T_{mp}}$ machine periods. Using the new model and stored inputs, a new energy consumption estimation $\hat{S}_{new}$ is calculated. The fit rate (5) is computed for both the $\hat{S}$ and $\hat{S}_{new}$, calculations, and chosen is the model with the best fit. If the new model fit-rate value is higher than that of the reference model, the reference model parameters will be updated accordingly.

4.4. Adaptive model predictive control design

Integrating the adaptive mechanism explained in Subsection 4.3, the controller was improved to obtain adaptive capabilities against changes in device energy consumption dynamics over time. The new control system block diagram is shown in Figure 4d, where the observer is replaced by the adaptive mechanism. When the adaptation law updates the reference model, the controller model will also be updated, while estimated current states are obtained from the reference model. Thusly, Algorithm 1 gathers all the main steps that the implementation of the control system must follow. Note that $c_{T_{mp}}$ is a counter that increments when the machine period ends, and when $c_{T_{mp}}$ equals $N_{T_{mp}}$, the adaptation strategy is executed, otherwise only the measurements are stored.

5. Energy efficiency improvements

The proposed approach was validated and compared with a RBC strategy – traditionally the most widely used controller for peripheral device management in industry – with the ability to pose or translate expert knowledge using natural language via decisions tree [31]. Initially, the machine used one RBC for each peripheral device. The following three scenarios were designed for the progressive replacement of each RBC and to be able to evaluate the yield of both approaches:

- *Scenario 1.* The proposed approaches (MPC and Adaptive MPC) only managed two peripheral devices, exclusively measuring the power consumption of the periodic process and peripheral devices P_1 and P_3.

- *Scenario 2.* The P_2 consumption was included, but the proposed approach handled the same peripheral devices as in the first scenario; this was because this scenario focused on evaluating the controller when no device was considered. Nonetheless, the consumption of this device should be viewed as a disturbance in the system output. Thus, the aim was to verify the capacity of the adaptive mechanism to reject disturbances and to explore how controller decisions could be affected.

- *Scenario 3.* The proposed approaches managed the three peripheral equipment, evaluating possible improvements in EE when all peripheral devices are smartly synchronized with the power consumption of the machining process.

Algorithm 1 Adaptive MPC scheme

Require: $\mathbf{U_{iden}}$ and $\mathbf{S_{iden}}$, the identification input-output data
Require: n, the model order

1: Compute the initial model

$$\hat{x}(k+1) = A\ \hat{x}(k) + B\ U(k)$$
$$\hat{S}(k) = C\ \hat{x}(k) + D\ U(k)$$

2: Start-up of the machine and control system
3: Sensor and reference model generate $S(k)$ and $\hat{S}(k)$, respectively
4: Adaptation law block receives and stores $U_s(k)$, $U_p(k)$, $S(k)$ and $\hat{S}(k)$, if k is the end of the machine period then $c_{T_{mp}} = c_{T_{mp}} + 1$
5: If the $c_{T_{mp}}$ is equal to $N_{T_{mp}}$, then let $c_{T_{mp}} = 0$ and go to step 6, otherwise go to step 9
6: A new model is calculated from stored measurements

$$\hat{x}_{new}(k+1) = A_{new}\ \hat{x}_{new}(k) + B_{new}\ U(k)$$
$$\hat{S}_{new}(k) = C_{new}\ \hat{x}_{new}(k) + D_{new}\ U(k)$$

and computes the $\hat{S}_{new}$
7: If $\gamma(S, \hat{S}_{new})$ is bigger than $\gamma(S, \hat{S})$ then, go to step 8, otherwise go to 9
8: The model used in both the controller and the reference model are updated with the new one
9: Controller computes $\hat{S}_s$ and executes the optimization problem
10: $U_p(k) = U_p^*(k|k)$ is established in peripheral equipment
11: If the process has finished then exit, otherwise go to step 3

All scenarios were designed to emulate a real production facility as closely as possible: the devices should experience progressive degradation pattern on energy consumption emulated by changing configurations. Figure 5 shows the initial and final energy consumption profiles for each energy profile. Note that emulated degradation behaviors are non-linear, not only to mimic a realistic scenario, but also to demonstrate the robustness of the proposed adaptive mechanism.

The EE and performance of the approaches were measured through the following KPIs:

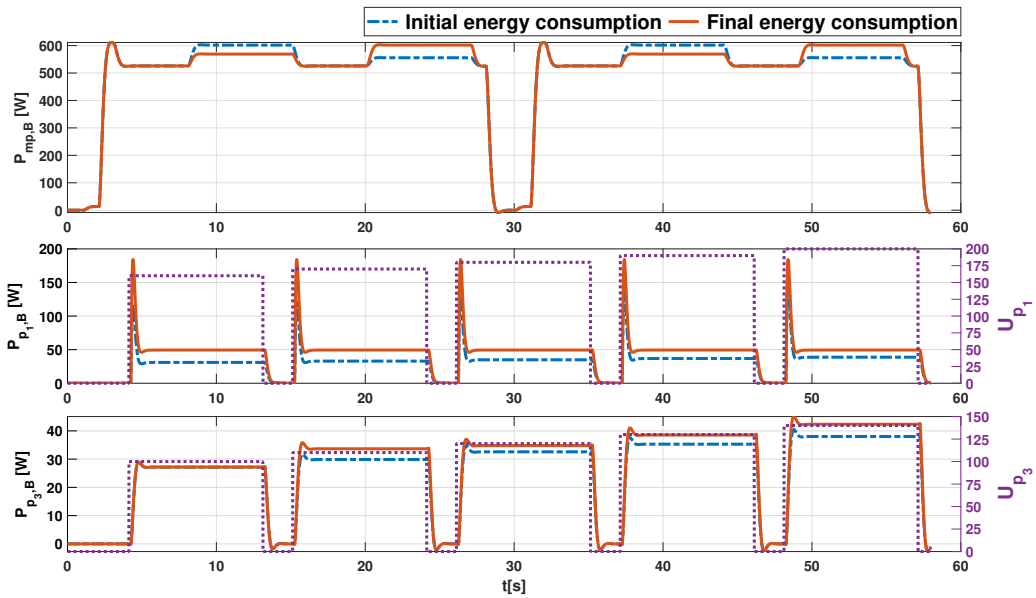

Figure 5: Emulation of degradation impact on energy consumption profiles.

(i) *Total electrical energy consumed.* This value represents the amount of energy that will be charged, so any energy savings will mean a monetary saving for the factory. According to IEEE Std 260.1-2004 [32], consumed electrical energy is measured in terms of Watt hour (Wh) and is expressed as

$$\mathbf{KPI}_1 = \frac{T_s}{3600} \sum_{k=0}^{N_{\mathbf{S}}} S(k), \tag{8}$$

where $S(k)$ is the real power consumed in instant k, T_s is the sampling time and $N_{\mathbf{S}}$ is the number of measurements made.

(ii) *Maximum peak.* Decreasing maximum consumption allows contracted energy capacity to be reduced, which in turn means cost savings and better management of available resources. It can be computed as

$$\mathbf{KPI}_2 = \|\mathbf{S}\|_\infty, \tag{9}$$

where $\mathbf{S} = [S(0), S(1), \ldots, S(N_{\mathbf{S}})]$ is the set of measurements made.

Table 1: KPI values for each approach and scenario.

KPI \ Controller		RBC		MPC			Adaptive MPC		
		$N_p = 2$	$N_p = 3$	Scenario 1	Scenario 2	Scenario 3	Scenario 1	Scenario 2	Scenario 3
$\mathbf{KPI}_1$: Energy consumption	[Wh]	752.50	796.66	748.33	791.66	794.16	738.33	785.83	780.36
$\mathbf{KPI}_2$: Maximum peak	[kW]	1.03	1.09	0.96	0.99	0.96	0.95	1.02	0.96
$\mathbf{KPI}_3$: Load factor	[%]	72.20	72.39	77.32	78.92	81.32	76.71	76.23	80.24
$\mathbf{KPI}_4$: Standard deviation	[W]	372.15	384.57	326.95	336.60	320.00	324.03	343.07	314.16

*N_p: the number of peripherals devices considered.

(iii) *Load factor.* This is the ratio between the energy consumed and the maximum energy demand contracted during a defined period (hours, days, weeks or months). The load factor is expressed as a percentage as follows:

$$\mathbf{KPI}_3 = 100 \, \frac{\mathbf{KPI}_1}{N_{\mathbf{S}} \, \mathbf{KPI}_2} \, \%, \tag{10}$$

where $N_{\mathbf{S}}$ $\mathbf{KPI}_2$ is energy consumption at maximum demand contracted in a period of $N_{\mathbf{S}}$ samples. A suitable load factor must be greater than 50% since it means that at least half the capacity is used.

(iv) *Standard deviation.* Energy consumption in an industrial process with low deviation represents an optimal use of resources, as it reflects the avoidance of power peaks and convergence to constant consumption. Standard deviation is defined as:

$$\mathbf{KPI}_4 = \sqrt{\frac{1}{N_{\mathbf{S}}} \sum_{k=0}^{N_{\mathbf{S}}} (S(k) - \mu_{\mathbf{S}})^2}, \tag{11}$$

where $\mu_{\mathbf{S}}$ is the mean value of energy consumption in an instant $S(k)$ and $N_{\mathbf{S}}$ is within a suitable time frame for analysis (greater than a machine period), in this case, one hour.

Each approach and scenario was executed 10 times and in 125 T_{mp}, representing an hour of machine work. The mean KPI values obtained are presented in Table 1, for a deviation of less than 5%. The KPI values obtained for both proposed approaches were an improvement over the RBC approach; with an energy saving of up to 16.3Wh, the maximum peak and standard deviation decreased by around 13 W and 96 W, respectively. Although the RBC strategy obtained a load factor value greater than 50%, which is desirable, both approaches proposed improved on that value by between 4% and 9%.

Table 2: Energy efficiency improvements.

KPI \ Controller	Efficiency [%]					
	MPC			Adaptive MPC		
	Scenario 1	Scenario 2	Scenario 3	Scenario 1	Scenario 2	Scenario 3
KPI$_1$: Energy consumption	0.55	0.63	0.31	1.89	1.36	2.04
KPI$_2$: Maximum peak	7.07	8.57	11.17	7.66	5.97	11.61
KPI$_3$: Load factor	7.08	9.06	12.34	6.24	5.34	10.85
KPI$_4$: Standard deviation	22.77	23.49	30.71	24.13	20.51	33.24

The EE gains using the proposed approach for each scenario are summarized in Table 2. Although the 2% energy saving may not seem to be very important in terms of quantity, it should be understood that the improvement was accomplished by changing the scheduling of peripheral devices without modifying device hardwares or machining sequences. The inclusion of an adaptive mechanism has managed to save more energy than keeping a computed model offline. When the controller has an updated model of the machine's current energy consumption, decision making is better. However, the adaptive approach sacrifices other KPIs to maximize energy savings and is more sensitive to disturbances. The MPC maintained a high load factor improvement and produced better results for scenario 2, when there were disturbances. The MPC is not sensitive to disturbances, however, because they have not been modeled, whereas in the adaptive approach, the measures used to generate new models online include disturbances. Finally, the best scenario in terms of maximizing performance is to manage all the peripheral devices (scenario 3).

Figure 6 depicts the profiles for four machine cycles when each approach managed all the peripheral devices. The reduction in high energy demand is appreciable and is, furthermore, intelligently distributed over time. Note how the proposed approaches activated peripheral devices when consumption for the machining process was lower. Although their decisions were very similar, the adaptive approach achieved lower consumption than the MPC approach, which depends on the reference model used by the controller. This explains why it is important to have an updated model that has been calculated with suitable parameters.

The adaptive approach achieved a fit greater than 80% in all the experiments. Two examples are shown in Figure 7a and 7c, of scenarios 2 and 3, respectively. In scenario 2, as the input P_2 was not considered, the identification method could not adequately model the corresponding energy profile. This was because, when P_2 was activated, there were no changes in the model

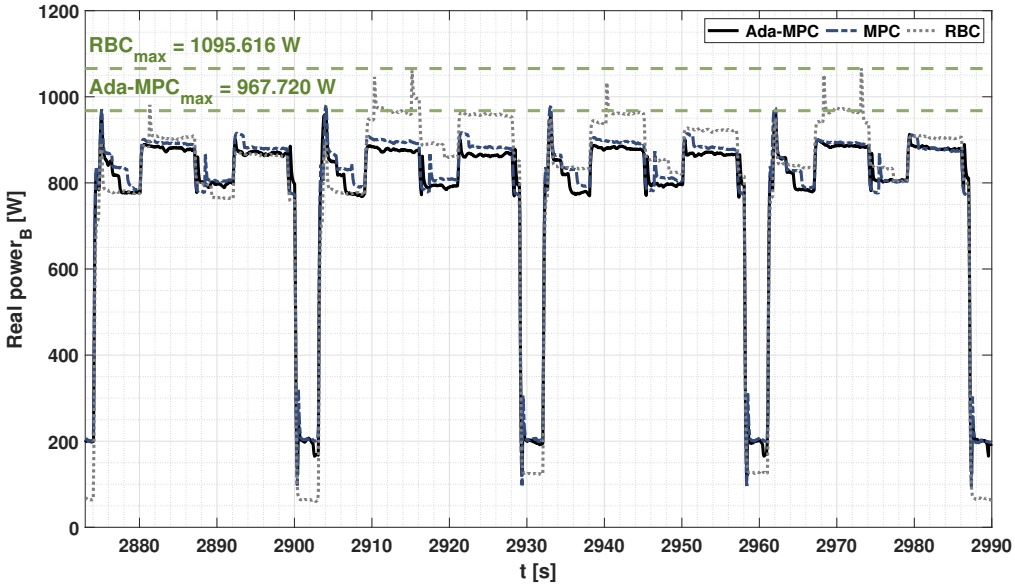

Figure 6: Energy profiles for each approach managing all peripheral devices.

output since the model inputs experienced no changes. Furthermore, an incorrect model with a high fit can be generated that assigns disturbance (P_2) consumption to other known devices, increasing steady-state error. When that happens, the reference model might be replaced by an incorrect model and the estimated consumption may deviate from real consumption in the ensuing machine periods. An example is displayed in Figure 7b at around 78 T_{mp}, where the evolution of the fit of the reference model, in each machine period, is presented without and with an adaptive approach. Note how the adaptive approach was rapidly self-adjusting and maintained a high fit. The fit of the MPC model deteriorated over time, while in most periods, the adaptive approach maintained a fit of over 80%.

For scenario 3, the adaptive mechanism provided a fit greater than 82% during the entire experiment for all the tests carried out; an example is shown in Figure 7c. Note that, during the production process, when the second cut was made in the material, there was some steady-state error due to nonlinearity between input and output that the linear model could not represent. Figure 7d shows how the adaptive approach that began with a model with high error converged to models with low error. Although the MPC and Ada-MPC started with the same reference model, the first fit for each approach

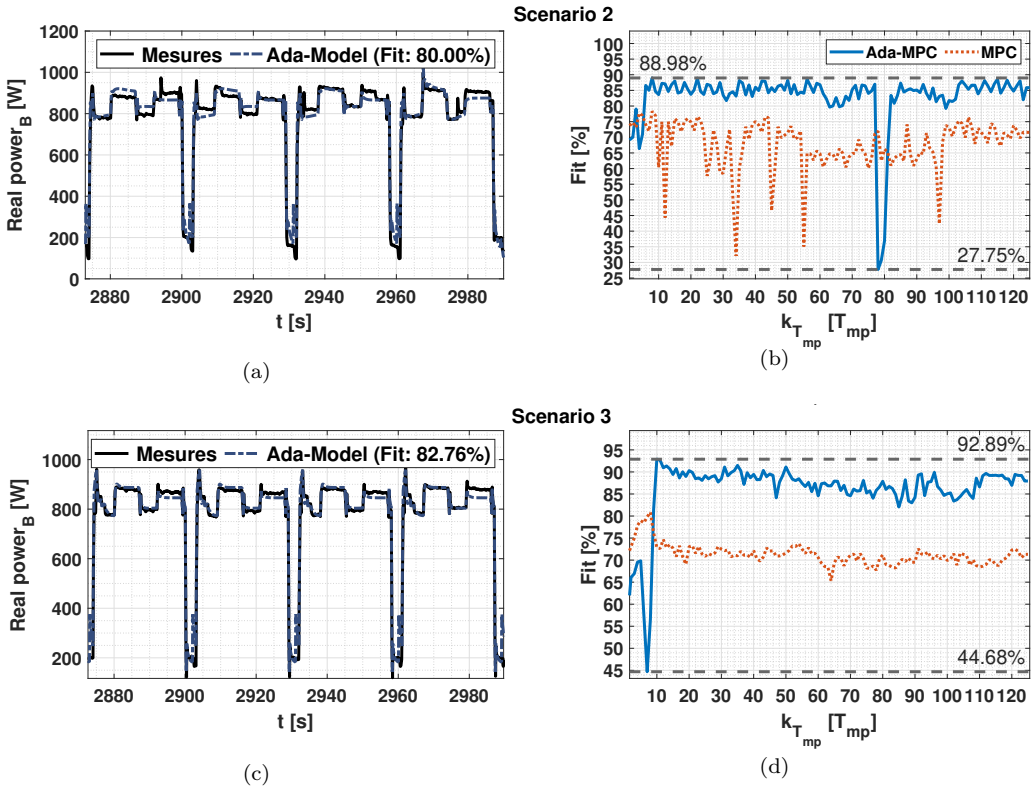

Figure 7: Adaptive mechanism performance. (a) and (c) Comparison of energy measurements with the reference model output. (b) and (d) Comparison of model fit evolution between the adaptive model and the model identified offline.

was very different, because this depended on the state of the machine or the environment, which changed energy consumption, especially the offset. Similar to what happened in scenario 2, the model used for MPC deteriorated over time, whilst the adaptive approach maintained fit at between 82% and 92%. These results show the ability of the proposed approach to adapt to changes in the consumption profile of the machine over time and the feasibility of carrying it out in real industrial applications.

6. Conclusions

A methodology to reduce the cost and environmental impact associated with the energy consumed by an industrial machine has been defined. The methodology is based on identification algorithms towards getting a linear data-driven model that generates a highly accurate (greater than 80%) machine energy model. With this energy model, an optimization-based controller with prediction features manages peripheral devices to maximize machine efficiency. The proposed controller minimizes the total power consumption while reducing the maximum power peak, ensuring efficient power consumption.

Since in an industrial production environment the constant operation of devices causes progressive device degradation and may lead to energy consumption dynamics changing over time, an adaptive mechanism is proposed to react to new dynamic behaviors, keeping the controller up-to-date. As a result, the estimated consumption will be close to the current consumption of the machine. The controller and adaptive mechanism were implemented in a real time and validated using the IIC testbed.

The proposed approach was compared with the widely used rule-based control approach, whose performance and energy efficiency were assessed using four key performance indicators. The validation was designed to progressively replace the rule-based control of each peripheral equipment, presenting three scenarios: the first scenario, the control system manages only two peripheral devices without measuring the consumption of the third. The second scenario, the consumption of the third peripheral was measured but the control system did not consider its input, performing as a disturbance. Finally, the third scenario, the control system manages all peripheral equipment. Furthermore, in all scenarios, the energy degradation of all devices was emulated by changing the configuration of each one.

In Scenario 2 (with disturbances), both the control and the adaptive mechanism demonstrate robustness against disturbances; the controller managed to save approximately 1.3% energy and reduce the maximum power peak by up to 5.9%, the adaptive mechanism ensured that the prediction had an fit rate of around 80 %. In scenario 3 (controlling all peripheral equipment), the controller saved around 2% of energy and reduced maximum consumption by up to 11%, and the adaptive mechanism converged to models with a fit rate greater than 82% over time. These results indicate that the proposed approach obtains better improvements by increasing the number of peripheral equipment to be managed and suitable robustness for industrial cases. Depending on the particular case, results may vary, but the findings here suggest that there is room for savings in terms of energy consumed, contracted capacity and penalties for high consumption. Taking into account that these improvements have been achieved without modifying or investing in new hardware.

With the meaningful results obtained, and in order to increase the robustness of the proposed approach, a delay estimator will be integrated into the adaptive mechanism, thus, high variations in input-output delay will be allowed. Furthermore, a modeling strategy should be developed to consider the typical input-output nonlinearities found in the power consumption of industrial machines. As well as, the proposed control system will be validated into the real industrial environment.

Acknowledgment

This work has been supported by the Doctorats Industrials program from the Catalan Gobernment (2019 DI 4). Authors would like to thank the companies of the Inzu Group, Etxe-tar, and Ikergune, for the support related to high-productivity systems.

References

[1] Mike Schulze, Henrik Nehler, Mikael Ottosson, and Patrik Thollander. Energy management in industry–a systematic review of previous findings and an integrative conceptual framework. *Journal of Cleaner Production*, 112:3692–3708, 2016.

[2] IEA. Electricity information 2019: Overview. url-http://www.iea.org/statistics/, 2019.

[3] Atabani Abdelaziz, Rahman Saidur, and Saad Mekhilef. A review on energy saving strategies in industrial sector. *Renewable and sustainable energy reviews*, 15(1):150–168, 2011.

[4] Dasheng Lee and Chin-Chi Cheng. Energy savings by energy management systems: A review. *Renewable and Sustainable Energy Reviews*, 56:760–777, 2016.

[5] John W Sutherland, David A Dornfeld, and Barbara S Linke. *Energy Efficient Manufacturing: Theory and Applications*. John Wiley & Sons, 2018.

[6] Yoon, Hae-Sung and Kim, Eun-Seob and Kim, Min-Soo and Lee, Jang-Yeob and Lee, Gyu-Bong and Ahn, Sung-Hoon. Towards greener machine tools–A review on energy saving strategies and technologies. *Renewable and Sustainable Energy Reviews*, 48:870–891, 2015.

[7] Anna Carina Roemer and Steffen Strassburger. A review of literature on simulation-based optimization of the energy efficiency in production. In *2016 Winter Simulation Conference (WSC)*, pages 1416–1427. IEEE, 2016.

[8] Markus Rager. *Energieorientierte Produktionsplanung: Analyse, Konzeption und Umsetzung*. Springer-Verlag, 2008.

[9] Jan Schlechtendahl, Philipp Eberspaecher, and Alexander Verl. Energy control system for energy-efficient control of machine tools. *Production Engineering*, 11(1):85–91, 2017.

[10] Jan-Peter Seevers, J Johst, Tim Weiß, Henning Meschede, and Jens Hesselbach. Automatic time series segmentation as the basis for unsupervised, non-intrusive load monitoring of machine tools. *Procedia CIRP*, 81:695–700, 2019.

[11] Seung-Jun Shin, Jungyub Woo, Sudarsan Rachuri, and Wonchul Seo. An energy-efficient process planning system using machine-monitoring data: A data analytics approach. *Computer-Aided Design*, 110:92–109, 2019.

[12] Jenny L Diaz and Carlos Ocampo-Martinez. Energy efficiency in discrete-manufacturing systems: insights, trends, and control strategies. *Journal of Manufacturing Systems*, 52:131–145, 2019.

[13] Alperen Can, Gregor Thiele, Jörg Krüger, Jessica Fisch, and Carsten Klemm. A practical approach to reduce energy consumption in a serial production environment by shutting down subsystems of a machine tool. *Procedia Manufacturing*, 33:343–350, 2019.

[14] Jan Schlechtendahl, Philipp Eberspächer, Philipp Schraml, Alexander Verl, and Eberhard Abele. Multi-level energy demand optimizer system for machine tool controls. *Procedia CIRP*, 41:783–788, 2016.

[15] David A Guerra-Zubiaga, Abdullah Al Mamun, and Germanico Gonzalez-Badillo. An energy consumption approach in a manufacturing process using design of experiments. *International Journal of Computer Integrated Manufacturing*, 31(11):1067–1077, 2018.

[16] Kotaro Mori, Benjamin Bergmann, Daisuke Kono, Berend Denkena, and Atsushi Matsubara. Energy efficiency improvement of machine tool spindle cooling system with on–off control. *CIRP Journal of Manufacturing Science and Technology*, 25:14–21, 2019.

[17] Taejung Kim, Taeho Kim, and Sungchul Jee. Standby strategies for energy saving in peripheral equipment of machine tools. *Journal of the Korean Society for Precision Engineering*, 30(5):486–492, 2013.

[18] Nancy Diaz, Seungchoun Choi, Moneer Helu, Yifen Chen, Stephen Jayanathan, Yusuke Yasui, Daeyoung Kong, Sushrut Pavanaskar, and David Dornfeld. Machine tool design and operation strategies for green manufacturing. In *Proceedings of 4th CIRP International Conference on High Performance Cutting*, 2010.

[19] Fysikopoulos Apostolos, Papacharalampopoulos Alexios, Pastras Georgios, Stavropoulos Panagiotis, and Chryssolouris George. Energy efficiency of manufacturing processes: a critical review. *Procedia CIRP*, 7: 628–633, 2013.

[20] Muhtar Ural Uluer, Hakki Ozgur Unver, Gozde Gok, Nilgun Fescioglu-Unver, and Sadik Engin Kilic. A framework for energy reduction in

manufacturing process chains (E-MPC) and a case study from the turkish household appliance industry. *Journal of Cleaner Production*, 112: 3342–3360, 2016.

[21] Andrea Cataldo, Andrea Perizzato, and Riccardo Scattolini. Production scheduling of parallel machines with model predictive control. *Control Engineering Practice*, 42:28–40, 2015.

[22] GY Zhao, ZY Liu, Y He, HJ Cao, and YB Guo. Energy consumption in machining: Classification, prediction, and reduction strategy. *Energy*, 133:142–157, 2017.

[23] IIC. Industrial internet consortium, 2020. URL `https://www.iiconsortium.org`.

[24] Jenny L Diaz, Miguel Bermeo, Javier Diaz-Rozo, and Carlos Ocampo-Martinez. An optimization-based control strategy for energy efficiency of discrete manufacturing systems. *ISA transactions*, 93:399–409, 2019.

[25] Lennart Ljung. Perspectives on system identification. *Annual Reviews in Control*, 34(1):1–12, 2010.

[26] Peter Van Overschee and Bart De Moor. *Subspace Identification for Linear Systems : Theory - Implementation - Applications*. Springer US, Boston, MA, 1996. ISBN 9781461304654.

[27] Miguel Bermeo-Ayerbe and Carlos Ocampo-Martinez. Energy consumption dynamical models for smart factories based on subspace identification methods. In *2019 IEEE 4rd Colombian Conference on Automatic Control (CCAC)*, pages 1–6. IEEE, 2019.

[28] Bernard Friedland. *Control system design: an introduction to state-space methods*. Courier Corporation, 2012.

[29] Igor V. Tetko, Věra Kůrková, Pavel Karpov, and Fabian Theis. *Artificial Neural Networks and Machine Learning-ICANN 2019: Deep Learning: 28th International Conference on Artificial Neural Networks, Munich, Germany, September 17-19, 2019, Proceedings*, volume 11728. Springer Nature, 2019.

[30] James Blake Rawlings and David Mayne. *Model Predictive Control: Theory and Design*. Nob Hill Publishing, Madison, WI (USA), 2009.

[31] Qianqian Zhong, Renzhong Tang, and Tao Peng. Decision rules for energy consumption minimization during material removal process in turning. *Journal of Cleaner Production*, 140:1819–1827, 2017.

[32] IEEE 260.1 Working Group et al. IEEE Standard Letter Symbols for Units of Measurement (SI Customary Inch-Pound Units, and Certain Other Units). *IEEE Std 260.1-2004 (Revision of IEEE Std 260.1-1993)*, pages 1–30, Sep. 2004. doi: 10.1109/IEEESTD.2004.94618.